Journal of Earth Science, Vol. 27, No. 4, p. 599–610, August 2016 *ISSN 1674-487X*
Printed in China
DOI: 10.1007/s12583-016-0715-3

Mineral Chemistry of Melanite from Calcitic Ijolite, the Oka Carbonatite Complex, Canada: Implications for Multi-Pulse Magma Mixing

Wei Chen*[1], Weiqi Zhang[1], Antonio Simonetti[2], Shaoyong Jiang[1, 3]

1. *State Key Laboratory of Geological Processes and Mineral Resources*, *China University of Geosciences*, *Wuhan* 430074, *China*
2. *Department of Civil & Environmental Engineering & Earth Sciences*, *University of Notre Dame*, *Notre Dame IN* 46556, *USA*
3. *State Key Laboratory for Mineral Deposits Research*, *School of Earth Sciences and Engineering*, *Nanjing University*, *Nanjing* 210093, *China*

ABSTRACT: Ti-rich garnet is found within calcitic ijolite from the Oka carbonatite complex in Canada, which is characterized by 58%–73% andradite component (2.12 wt.%–4.18 wt.% TiO_2) and classified as melanite. The garnet displays complex zoning and contains abundant high field strength elements (HFSEs) and rare earth elements (REEs). Three groups (I, II, III) have been identified based on their petrographic nature. Compared to groups II and III, Group I garnet cores contain higher TiO_2, MgO, HFSE, and REE and lower SiO_2 abundances. The distinct chemical and petrographic signatures of the investigated garnets cannot be attributed to simple closed system crystallization, but they are consistent with the multi-pulse magma mixing. Combined with previously reported U-Pb ages for apatite from the calcitic ijolite, at least three stages of magma evolution and subsequent mixing have been involved in the generation of calcitic ijolite at Oka. The early-formed melt that generated Group I garnet core was later mixed with at least two small-volume, more evolved melts. The intermediate stage melt formed the remaining garnet along with some pyroxene, calcite, nepheline, and apatite at 127±3.6 Ma. The youngest, most evolved melt generated the majority of pyroxene, calcite, nepheline, and apatite within the calcitic ijolite at 115±3.1 Ma.

KEY WORDS: melanite garnet, calcitic ijolite, Oka, magma mixing.

0 INTRODUCTION

The Oka intrusive carbonatite complex (Fig. 1) comprises a broad spectrum of rocks, including carbonatite, okaite, ijolite, calcitic ijolite, jacupirangite, and alnöite. Previous chemical, isotopic, and geochronological investigations of the carbonatite and associated silicate rocks from Oka indicate the involvement of periodic generation of small volume, partial melts from a heterogeneous mantle plume and subsequent magma mixing (Chen and Simonetti, 2014, 2013; Chen et al., 2013; Zurevinski and Mitchell, 2004). In addition, liquid immiscibility has been proposed for the formation of the carbonatite and associated silicate rocks at Oka (Treiman and Essene, 1985; Eby, 1975). Garnet dominated calcitic ijolite, which represents the most 'hybrid' carbonate-silicate suite of rocks at Oka, occurs solely proximal to the nature center (Fig. 1) and is the only rock type containing garnet within the complex.

Titanium-rich garnets commonly consist of andradite ($Ca_3Fe_2^{3+}Si_3O_{12}$), schorlomite ($Ca_3Ti_2[Al>Fe^{3+}]_2SiO_{12}$) or melanite ($Ca_3Ti_2[Al<Fe^{3+}]_2SiO_{12}$), and have been found within various extrusive and intrusive Si-undersaturated alkaline igneous rocks and related rock types (e.g., Niu et al., 2008; Chakhmouradian and McCammon, 2005; Vuorinen et al., 2005; Gwalani et al., 2000; Dingwell and Brearley, 1985; Manning and Harris, 1970). The garnets occurring in skarns and serpentinized peridotite bodies are interpreted to be of metamorphic or metasomatic origin (Russell et al., 1999; Dingwell and Brearley, 1985; Deer et al., 1982). Primary magmatic Ti-rich garnet forms in a wide range of pressure-temperature conditions with low Si-activities and oxygen fugacities (Vuorinen et al., 2005; Gwalani et al., 2000). Moreover, Ti-andradite phenocrysts within tephrite from the Amba Dongar carbonatite complex display complicated zonation, which suggests the involvement of polybaric differentiation, magma mixing, and kinetic effects in its formation history (Gwalani et al., 2000). Titanium-rich garnets from the Alnö complex show decreasing Ti but increasing Si within pyroxenite, ijolite, and nepheline syenite, which has been attributed to melt differentiation and small volume primitive magma mixing (Vuorinen et al., 2005).

In order to obtain a more detailed petrogenetic history of the associated silicate rocks within the Oka carbonatite complex, we investigate here the mineral chemistry and chemical zoning of garnets contained within calcitic ijolite from Oka, Québec (Canada). Given the distinct and unique 'hybrid' nature

*Corresponding author: wchen@cug.edu.cn

Manuscript received September 17, 2015.
Manuscript accepted November 23, 2015.

Chen, W., Zhang, W. Q., Simonetti, A., et al., 2016. Mineral Chemistry of Melanite from Calcitic Ijolite, the Oka Carbonatite Complex, Canada: Implications for Multi-Pulse Magma Mixing. *Journal of Earth Science*, 27(4): 599–610. doi:10.1007/s12583-016-0715-3. http://en.earth-science.net

of the calcitic ijolite suite rocks at Oka, investigation of the garnet chemistry included within this rock type will provide additional insights into the petrogenetic relationship between carbonatites and the alkaline silicate rocks as well as multiple stages of magma mixing. Lastly, the major and trace element results reported here are combined with existing geochronological data to formulate a more detailed temporal evolutionary history for the Oka complex.

1 GEOLOGICAL SETTINGS AND SAMPLE DESCRIPTIONS

The Oka carbonatite complex (Fig. 1) represents the most westerly alkaline intrusion and the sole occurrence of carbonatite within the Monteregian igneous province (MIP), which consists of nine alkaline intrusions and associated dikes in southeastern Québec, Canada. The carbonatite and associated alkaline silicate rocks of the Oka complex intruded Precambrian basement. Oka demonstrates a distorted figure eight structures with the northern and southern rings shown in the geological map (Fig. 1). Each ring consists of an early, outer annulus of alkaline silicate rocks and cored by later central carbonatites. Carbonatite in the Oka complex is predominantly coarse-grained calciocarbonatite, and contains accessory minerals such as biotite, apatite, nepheline, melilite, pyrochlore, perovskite, niocalite, magnetite, wollastonite, richterite, pyrite, Na-augite, and pyrrhotite (Chen and Simonetti, 2013; Gold et al., 1986). Okaite is composed of 60%–90% melilite, 10%–40% nepheline and minor amounts of haüyne, perovskite, apatite, biotite, magnetite, and calcite (Chen and Simonetti, 2013; Gold et al., 1986). Jacupirangite consists of fassaite and minor magnetite in a cumulate texture with interstitial melilite, calcite, and haüyne (Gold et al., 1986; Treiman and Essene, 1985). Ijolite at Oka encompasses a wide range of mafic rock types and contains clinopyroxene, melilite, nepheline, garnet, wollastonite or pectolite. Two Ti-garnet-bearing calcitic ijolite samples are investigated in this study (i.e., Oka21and Oka31), which consist of 30%–40% garnet, 25%–30% clinopyroxene, 20%–30% nepheline, and 5%–10% calcite as the major minerals and accessory apatite (Chen and Simonetti, 2013; Gold et al., 1986). The intimate mixture of ijolite and carbonatite exists in some portions of the Oka complex, which was interpreted as large ocelli of ijolite melt within carbonatite magma (Gold et al., 1986; Treiman and Essene, 1985).

Three groups of garnet have been identified within samples Oka21 and Oka31 based on their petrographic features. Group I garnet from Oka21 commonly displays distinct zonation, with a dark brown inclusion-poor core and a light brown inclusion-rich rim (Fig. 2a). Group II garnets are light brown and inclusion-rich as single, small grains within Oka21 and Oka31 (Fig. 2d). Group III garnet from Oka31 is light brown and inclusion-rich with weak oscillatory zonation (Fig. 2c). Clinopyroxene from both samples are light green in color and contain abundant inclusions (Figs. 2b, 2d). The mineral inclusions within light brown Ti-garnet include clinopyroxene, calcite, nepheline, and apatite. Those included within clinopyroxene consist of garnet, calcite, nepheline, and apatite. Calcite and nepheline are intergranular and occur mostly in the matrix. Apatite in calcitic ijolite is either intergranular or intragranular and commonly contains fluid/melt inclusions.

2 ANALYTICAL METHODS

The major element compositions of garnet were obtained using a Cameca SX50 electron microprobe analyzer (EMPA) at the University of Chicago. The EMPA is equipped with 4 wavelength-dispersive spectrometers and a high-resolution energy-dispersive solid-state detector. The EMP analyses were conducted using a 15 kV accelerating potential and 30 nA incident current for the garnet. The natural and synthetic mineral and glass standards employed for calibration purposes were: natural olivine (for Fe, Mn, Mg, and Si), natural albite (for Na), synthetic glass of anorthite composition (for Al, Ca), natural microcline (for K), and synthetic TiO_2 (for Ti). Calculated mineral formulae were normalized by stoichiometry.

In-situ trace element analyses of individual garnet grains were obtained using a UP213 nm laser ablation system coupled to a Thermo-Finnigan Element 2 sector field high-resolution ICP-MS. The NIST SRM 612 international glass standard was used for external calibration and ^{43}Ca ion signal intensities were employed as the internal standard to monitor instrumental drift. The content of CaO (wt.%) was obtained using EMPA.

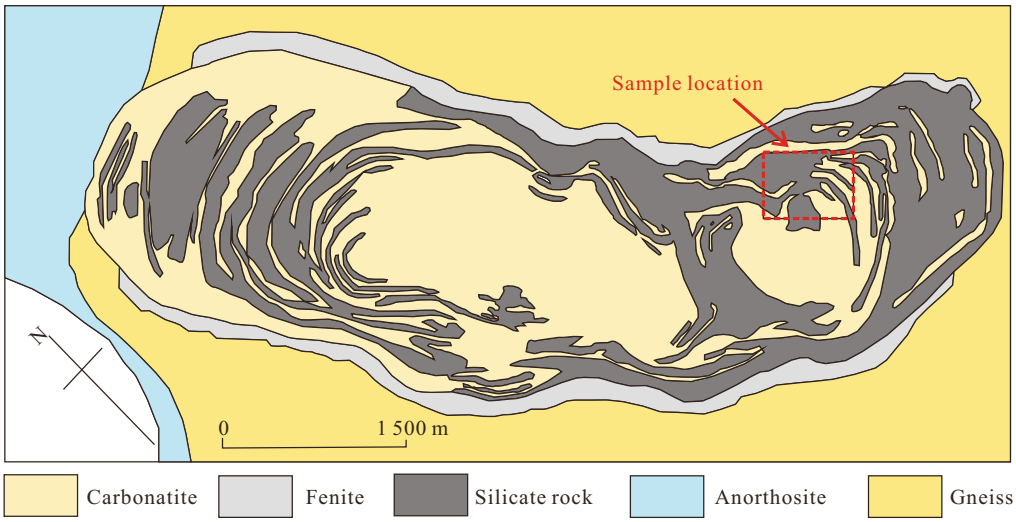

Figure 1. Detailed geological map of the Oka carbonatite complex (after Chen and Simonetti, 2013; Gold, 1972).

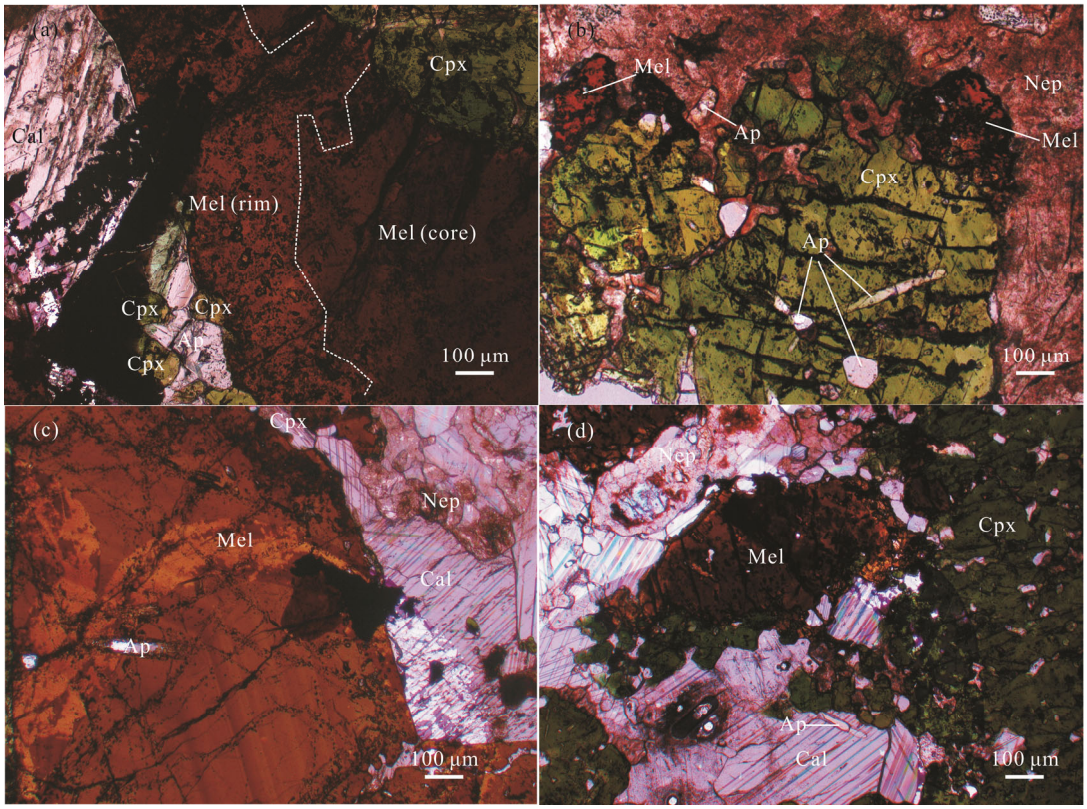

Figure 2. Petrographic images of samples investigated. (a) Zoned garnet from Oka21; (b) matrix garnet from Oka21; (c) huge oscillatory zoned garnet crystal from Oka31; (d) clinopyroxene from Oka31; Cpx. clinopyroxene, Mel. melanite, Ap. apatite, Cal. calcite, Nep. nepheline.

The standard and sample grains were ablated using a 25–100 μm spot size, 4–5 Hz repetition rate, and an energy density of ~10–12 J/cm^2. Analyses were conducted in a He atmosphere (0.7 to 1.0 L/min) within the ablation cell, and mixed with Ar (0.6 to 1.0 L/min) prior to entering the torch assembly. A typical analysis consisted of a ~60 s background measurement followed by data acquisition and ablation for ~60 s using a rapid peak jumping and dwell time of 8 ms for each element reported. Data reduction, including concentration determinations, method detection limits, and internal uncertainties were obtained using the GLITTER laser ablation data reduction software (van Achterbergh et al., 2001).

3 RESULTS

3.1 Garnet Mineral Chemistry

Garnet occurs as granular crystals in calcitic ijolite at Oka, with grain size range between 5 mm and 1.5 cm. Group I garnet within Oka21 show distinct zonation with color differences (i.e., light to dark brown; Fig. 2a). The oscillatory zoned Group III garnet demonstrates the light-golden-dark brown color band (Fig. 2c). Differences in color have been attributed to the variation of Ti contents in garnet, i.e., the dark zones are characterized by higher Ti abundances as suggested by Dingwell and Brearley (1985). This conclusion is further confirmed in this study since major element compositions reported here indicate that the dark-brown cores consist of higher TiO_2 contents (~4.8 wt.%) compared to those for the light-brown rims in Group I garnet (~2.8 wt.%; Fig. 2a; Table 1). It is also worthwhile to note that the rim of Group I garnet typically hosts abundant mineral inclusions (i.e., apatite, calcite, clinopyroxene, nepheline, and magnetite) and tiny multi-phase inclusions (10–20 μm; Figs. 2a, 2c).

The garnet formulae were normalized to 12 oxygens and 8 cations as shown in Table 1. The data demonstrate that Fe, Al, Si and Ti contents are varied, and the garnets contain varied contents of different end-members within the garnet group (i.e., andradite, grosullar, pyrope and spessartite; Locock, 2008; Table 1; Fig. 3). The andradite component (59.8%–73.0%) is the most dominant end-member for the analyzed garnet,

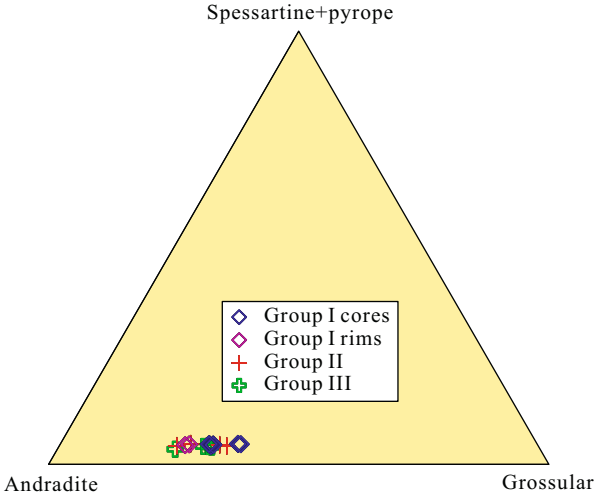

Figure 3. Compositional range of garnets in the andradite-grossular-spessartine+pyrope plot.

Table 1 Major element compositions for garnet within calcitic ijolite

Title	Group	Major elements (wt.%)										Formula units based on 12 anions										End members (%)		
		MgO	Al_2O_3	SiO_2	CaO	TiO_2	V_2O_3	MnO	Fe_2O_3	ZrO_2	Total	Mg	Al	Si	Ca	Ti	V	Mn	Fe	Zr	Si	Sps+ Prp	Grs	Ti-Adr
21 GNT 1	I-core	0.66	5.47	34.53	32.11	4.43	0.40	0.83	20.98	0.33	99.75	0.08	0.53	2.84	2.83	0.27	0.03	0.06	1.30	0.01	2.84	4.7	14.0	81.4
21 GNT 1-2	I-core	0.57	5.44	34.04	32.34	4.09	0.40	0.80	20.99	0.30	98.97	0.07	0.53	2.83	2.88	0.26	0.03	0.06	1.31	0.01	2.83	4.2	13.7	82.1
21 GNT 4-1	I-rim	0.52	5.17	34.62	32.08	2.87	0.39	1.05	22.22	0.22	99.14	0.06	0.51	2.88	2.85	0.18	0.03	0.07	1.39	0.01	2.88	4.6	14.5	80.9
21 GNT 2	II	0.44	4.22	34.79	31.87	2.22	0.32	0.88	23.32	0.15	98.21	0.06	0.42	2.92	2.87	0.14	0.02	0.06	1.48	0.01	2.92	4.0	13.2	82.9
21 GNT 3	II	0.42	4.38	34.94	31.78	2.44	0.34	1.07	22.76	0.19	98.31	0.05	0.43	2.93	2.85	0.15	0.02	0.08	1.44	0.01	2.93	4.3	13.9	81.8
21 GNT 4-2	I-core	0.68	5.39	33.36	31.78	4.81	0.45	0.74	20.71	0.36	98.27	0.09	0.53	2.79	2.85	0.30	0.03	0.05	1.30	0.01	2.79	4.6	11.6	83.8
21 GNT 4-3	I-core	0.67	5.36	33.87	32.35	4.37	0.38	0.81	20.85	0.32	98.97	0.08	0.52	2.81	2.88	0.27	0.03	0.06	1.30	0.01	2.81	4.6	12.2	83.2
21 GNT 4-4	I-core	0.61	5.38	33.78	32.29	4.54	0.40	0.84	21.10	0.31	99.24	0.08	0.53	2.80	2.87	0.28	0.03	0.06	1.32	0.01	2.80	4.5	11.9	83.7
21 GNT 4-5	I-core	0.63	5.35	33.41	32.19	4.29	0.41	0.78	20.74	0.30	98.11	0.08	0.53	2.80	2.89	0.27	0.03	0.06	1.31	0.01	2.80	4.4	12.0	83.5
21 GMT4-6	I-rim	0.55	4.54	33.72	32.00	3.70	0.39	0.91	22.40	0.32	98.53	0.07	0.45	2.83	2.88	0.23	0.03	0.06	1.42	0.01	2.83	4.4	9.5	86.1
21 GNT 5	II	0.56	4.59	34.98	31.92	3.39	0.41	1.03	22.02	0.26	99.15	0.07	0.45	2.90	2.84	0.21	0.03	0.07	1.37	0.01	2.90	4.8	12.9	82.4
31 GNT 1	II	0.55	5.91	34.91	32.29	2.65	0.29	0.88	21.84	0.17	99.50	0.07	0.57	2.88	2.85	0.16	0.02	0.06	1.35	0.01	2.88	4.3	18.4	77.3
31 GNT 2	II	0.42	4.14	34.58	32.09	2.96	0.40	0.86	23.51	0.25	99.21	0.05	0.41	2.88	2.87	0.19	0.03	0.06	1.48	0.01	2.88	3.8	10.8	85.4
31 GNT 3	II	0.43	4.18	34.45	32.87	2.96	0.37	0.81	23.73	0.19	99.98	0.05	0.41	2.86	2.92	0.18	0.02	0.06	1.48	0.01	2.86	3.6	9.5	86.9
31 GNT 5	II	0.44	3.84	34.27	32.38	3.45	0.42	0.85	23.97	0.19	99.82	0.05	0.38	2.85	2.88	0.22	0.03	0.06	1.50	0.01	2.85	3.8	7.5	88.7
31 GNT 4-1	III	0.53	5.83	34.97	32.66	2.59	0.30	0.86	21.11	0.21	99.07	0.07	0.57	2.89	2.90	0.16	0.02	0.06	1.31	0.01	2.89	4.2	18.7	77.1
31 GNT 4-2	III	0.53	6.07	34.57	32.54	2.70	0.32	0.78	21.04	0.22	98.76	0.07	0.59	2.87	2.89	0.17	0.02	0.05	1.31	0.01	2.87	4.0	19.1	77.0
31 GNT 4-3	III	0.55	6.14	34.96	32.45	2.61	0.34	0.85	21.10	0.17	99.17	0.07	0.60	2.89	2.87	0.16	0.02	0.06	1.31	0.01	2.89	4.2	19.9	75.8
31 GNT 4-4	III	0.53	6.10	34.54	32.38	2.51	0.34	0.84	21.47	0.17	98.87	0.07	0.60	2.87	2.88	0.16	0.02	0.06	1.34	0.01	2.87	4.2	18.9	76.9
31 GNT 4-5	III	0.55	5.78	35.07	32.34	2.67	0.34	0.88	21.10	0.17	98.90	0.07	0.56	2.90	2.87	0.17	0.02	0.06	1.31	0.01	2.90	4.3	19.1	76.6
31 GNT 4-6	III	0.50	6.27	34.99	32.10	2.63	0.34	0.86	20.95	0.18	98.80	0.06	0.61	2.89	2.84	0.16	0.02	0.06	1.30	0.01	2.89	4.1	21.4	74.5
31 GNT 4-7	III	0.36	4.77	35.31	32.41	2.12	0.32	0.85	23.26	0.11	99.52	0.04	0.47	2.92	2.87	0.13	0.02	0.06	1.45	0.00	2.92	3.5	16.0	80.5

Sps. Spessartine; Prp. pyrope; Grs. grossular; Ti-Adr. Ti-andradite.

whereas they contain low MgO and MnO contents and consistent with small proportions of pyrope (1.5%–2.9%) and spessartite (1.8%–2.5%; Table 1; Fig. 3). The grossular component varies between 7% and 21% in the analyzed garnet (Table 1; Fig. 3). In addition, these garnets are characterized by high TiO_2 contents (2.12 wt.%–4.81 wt.%), which is consistent with that found in melanite and schorlomite depending on whether Fe^{3+} or Ti dominates in the octahedral site (e.g., Chakhmouradian and McCammon, 2005; Deer et al., 1982). Since their TiO_2 compositions are <15 wt.%, garnet within calcitic ijolite is designated as melanite (Table 1; Saha et al., 2011; Deer et al., 1982).

The stoichiometry and site assignment of cations in melanite garnet remain a problem due to the uncertainty of Fe, Al and Ti substitutions in the tetrahedral site within the crystal structure (e.g., Chakhmouradian and McCammon, 2005; Dunworth and Bell, 2003; Armbruster et al., 1998; Locock et al., 1995; Dingwell and Brearly, 1985; Huggins et al., 1977a, b). The spectroscopic data indicate that the cation preference in the tetrahedral site within melanite garnet to be $Al \geq Fe^{3+} > Ti$ (e.g., Chakhmouradian and McCammon, 2005; Locock et al., 1995; Huggins et al., 1977a), whereas Huggins et al. (1977b) and Armbruster et al. (1998) stated that the Ti-Si exchange can be the predominant manner in which Ti is introduced into the garnet structure. Figure 4c shows a good negative correlation between SiO_2 and TiO_2 contents for the Oka melanite together with the worldwide magmatic Ti-garnets (R^2=0.95). These include melanite from the Crowsnest volcanic rocks (Dingwell and Brearley, 1985), the Amba Dongar carbonatite-alkalic complex (Gwalani et al., 2000), the Rugged Mountain (Russell et al., 1999), the Alnö complex (Vuorinen et al., 2005), and the Ti-garnets from the active Oldoinyo Lengainatro carbonatite volcano (Dawson, 1998; Dawson et al., 1995). The negative linear correlation between Ti and Si supports Ti substitution within the tetrahedral site as the predominant manner. Therefore, for this study, all Ti has been assigned into the tetrahedral site for the stoichiometry calculations. Figures 4a and 4b demonstrate the chemical compositions for melanite from Oka and these are compared to those from other alkaline complexes, which indicates that the former contains the lowest TiO_2 but the highest Al_2O_3 contents.

Relatively similar trace element patterns have been identified for all of the melanite grains investigated here (Fig. 5; Table 2). They show different degrees of REE enrichment (e.g., ~1 200 ppm to ~1 900 ppm). In general, Group I cores show the highest enrichment of REEs compared to the remaining garnets (Fig. 5; Table 2). The chondrite normalized REE patterns are upward convex and peak at Nd and Sm. The slope of the trends from Sm to HREEs (heavy REEs) is relatively flat, whereas a steeper slope is observed for the LREEs (light REEs) from Nd to La (Fig. 5a). Similar REE distribution patterns have been documented in garnet within melteigite, ijolite, and nepheline syenite from Alnö Island (Sweden; Vuorinen et al., 2005), clinopyroxenite and ijolite from the Sung Valley alkaline complex (northeastern India; Melluso et al., 2010), and plutonic rocks of the Eocene Tamazeght complex (Morocco; Marks et al., 2008), though different degrees in the REE enrichment are noted (Fig. 5a). Trace element plots indicate higher contents of Zr and Ta and depletions of LREEs, Hf, Ti, and Nb (Fig. 5b). The

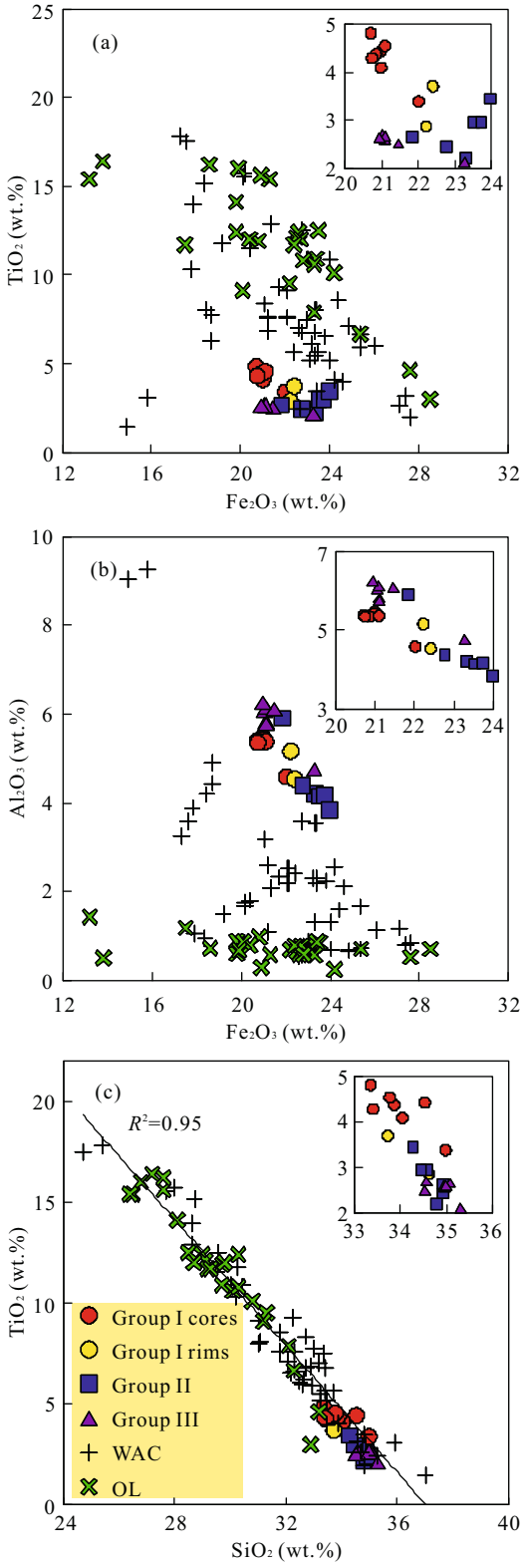

Figure 4. Major element variation plots for garnet from groups I, II and III. (a) TiO_2 vs. Fe_2O_3; (b) Al_2O_3 vs. Fe_2O_3; (c) TiO_2 vs. SiO_2. The chemical data of Ti-rich garnets from worldwide alkaline complex are referred to Maitra et al., 2011; Holub et al., 2010; Melluso et al., 2010; Vuorinen et al., 2005; Gwalani et al., 2000; Dawson, 1998; Dawson et al., 1995; Dingwell and Brearley, 1985. WAS. Worldwide alkaline complex; OL. Oldoinyo Lengai.

Table 2 Trace element compositions for garnet within calcitic ijolite

Sample	Group	Y	Zr	Nb	Ba	La	Ce	Pr	Nd	Sm	Eu	Gd	Tb	Dy	Ho	Er	Tm	Yb	Lu	Hf	Ta	Th	U
21 GNT 1	I-core	714	1 542	1 139	1.04	42.18	310.3	70.14	489.4	155.4	58.96	166.8	24.2	154.3	28.42	78.62	10.97	70.58	8.99	7.81	385.3	26.4	12.37
21 GNT 1-2	I-core	893	2 056	1 519	13.76	47.88	336	76.41	541.5	176.4	64.66	199.9	29.48	191.8	35.95	100.2	13.18	87.89	11.26	11.8	550.2	34.09	13.46
21 GNT 4-1	I-rim	715	1 389	426	25.65	27.98	224.1	57.43	426.6	149.8	56.09	161.3	24.04	148.6	27.29	73.12	9.54	62.66	8.54	8.82	127.4	16.27	15.36
21 GNT 4-2	I-core	812	2 065	1 468	11.22	46.72	329.8	76.62	531.8	168.8	64.93	192.5	27.16	172.5	32.28	88.67	12.24	75.73	10.33	14.37	400.1	31.63	14.51
21 GNT 4-3	I-core	813	2 087	1 624	0.67	47.38	343.3	79.47	538.9	173.1	64.9	185.9	27.51	175.9	32.52	90.1	12.41	78.93	10.02	14.3	538.3	33.57	14.88
21 GNT 4-4	I-core	613	1 417	1 191	7.62	46.94	326.6	76.26	504.3	147.9	54.74	147.2	21.24	131.8	23.6	64.15	8.64	55.81	7.49	7.14	343.9	27.72	12.93
21 GNT 4-5	I-core	920	2 180	1 526	78.14	51.87	333.3	81.04	556.5	177.2	66.48	201.9	30.37	195.5	37.03	99.48	13.88	88.85	11.64	11.89	539.7	31.39	13.41
21 GMT4-6	I-rim	769	1 650	643	2.86	29.41	244.9	64.49	472.7	161.3	61.98	178.2	26.45	162.1	29.26	78.4	10.71	67.88	8.88	9.3	241.2	27.74	21.54
21 GNT 2	II	498	798	405	1.21	29.11	258.6	61.24	420.7	137.1	54.48	131.4	18.12	106.4	18.28	48.67	6.39	41.37	5.41	3.03	73.68	11.89	10.27
21 GNT 3	II	675	1 165	591	108.17	46.55	285.8	69.14	474	155.1	59.38	160.3	23.3	140.4	25.99	72.25	9.57	63.08	8.12	6.42	138.5	15.64	12.32
21 GNT 5	II	653	1 251	579	6.21	41.25	248.2	66.24	467.8	155.8	62.28	158.3	23.52	138.3	24.85	64.87	8.81	59.18	7.23	7.22	140	19.15	16.71
31 GNT 1	II	606	1 052	647	0.69	34.69	270.7	66.77	459.1	159.5	56.64	145.7	21.56	124.9	23.41	60.42	8.25	54.65	7.41	4.28	148.8	20.53	12.11
31 GNT 2	II	647	1 853	594	2.09	27.9	207.3	55.29	410.6	153	50.75	156.1	23.07	130.3	23.41	60.14	8.04	50.66	7.05	9.5	177	39.94	20.03
31 GNT 3	II	568	1 189	536	0.85	29.51	247.2	63.94	444.2	162.1	56.84	143.1	20.9	116.9	21.26	52.41	7.34	49.67	6.41	5.85	152.6	16.36	23.07
31 GNT 5	II	458	1 298	700	10.55	28.09	239.1	60.81	388.3	142.4	51.38	120.5	18.02	90.61	15.8	39.22	5.1	35.67	4.51	5.27	135.8	25.63	12.81
31 GNT 4-1	III	642	1 071	404	0.65	37.07	280.3	69.79	447	157.1	55.81	149.9	22.65	131.1	23.41	61.81	8.69	56.41	7.5	4.52	124	18.64	10.47
31 GNT 4-2	III	651	1 133	369	101.18	40.17	258.6	63.22	438.9	154.8	55.3	148.7	23	130.4	23.85	62.06	8.61	54.15	7.58	5.07	110.1	20.34	9.87
31 GNT 4-3	III	762	1 423	520	1.04	40.4	291.9	72.25	481.2	171.6	60.34	172.8	26.11	150.7	28.18	71.73	10.06	65.53	8.97	5.83	168.3	26.99	11.72
31 GNT 4-4	III	709	1 263	511	0.69	37.12	282	68.94	456.6	162	57.34	162.7	24.56	141.4	26.95	69.65	9.53	64.44	8.66	5.07	167.4	23.43	11.4
31 GNT 4-5	III	690	1 135	389	1.43	35.16	265.4	66.6	439.5	162	58.25	157.5	23.69	134.6	25.36	64.37	9.42	60.33	7.28	4.51	103.8	20.06	10.27
31 GNT 4-6	III	675	1 269	502	1.1	33.66	255.5	62.69	418.7	149.3	53.32	149.8	22.74	132.7	24.92	66.08	9.04	60.43	7.87	5.98	157.8	22.07	10.62
31 GNT 4-7	III	661	1 249	394	2.46	32.25	251.4	64.19	409.9	153	54.06	147.8	22.75	128.1	24.32	61.65	8.79	56.18	7.77	7.73	114.8	24.21	11.66

Note: Concentrations are presented in ppm.

behavior of U is more complicated, which indicates a trivial enrichment in some garnet grains (groups II and III) relative to the Group I garnet (Fig. 5b).

3.2 Zoning Profiles

Based on optical and compositional properties, Group I garnet within Oka21 consists of two zones with sharp discontinuity; an inner dark-brown core surrounded by a golden-brown rim (e.g., Fig. 2a). Group III garnet from Oka31 shows fine-scale oscillatory zonation with weak color differences (e.g., Fig. 2c). Two representative grains from both groups have been investigated in detail (i.e., core-to-rim variations) and the elemental abundances are shown in Fig. 6.

The compositional variation range for Group I is the largest amongst the analyzed garnet grains. As shown in the major and trace element composition traverse plots (Fig. 6), both TiO_2 and MgO contents of the garnet decrease from core to rim. In contrast, the abundances of other major elements such as Fe, Si, and Mn increase from core to rim. This is consistent with the coupled substitutions of Ti-Si and Mg-Mn in the tetrahedral and octahedral sites, respectively (e.g., Fig. 4c). As for the trace element variations within the zoned garnet, Group I shows depletion of HFSEs (e.g., Hf, Zr) and HREEs in the light-brown rim relative to the core. Moreover, the ratios of La/Lu and Th/U are low in the rim as well (Fig. 6). The chemical variation in Group III is not as prevalent as that recorded in Group I garnet. However, no distinct chemical trends could be identified that match the oscillatory patterns for Group III garnet shown in Fig. 2.

Of note, the chemical compositions of Group II and the oscillatory zoned Group III garnets are similar to the rim compositions with Ti depletion for Group I garnet (Tables 1, 2; Fig. 7). In addition, these Ti-depleted garnets contain low abundances of other HFSEs (e.g., Zr, Hf, Nb, Ta), HREEs compared to the dark-brown core from Group I (Figs. 7 & 8c). The positive correlations between Ti and other HFSEs suggest similar geochemical behavior in the garnet formation processes (Fig. 7).

4 DISCUSSION

4.1 Trace Element Distribution

The chemical composition results obtained here for melanite indicate REE enrichment (~1 300 ppm to 1 900 ppm). Compared to other rock forming minerals within the calcitic ijolite (e.g.,

Table 3 Trace element distributions among major mineral phases from Oka21 and Oka31

	Th	U	Th/U	Zr	Hf	Zr/Hf	LREE	LREE%	MREE	MREE%	HREE	HREE%	$(La/Gd)_N$	$(La/Lu)_N$
Ap 21	956	48.6	19.7				21 804	74.21	560	11.93	22	1.9	33.04	796.44
Ap 31	1 071	55.5	19.3				21 686	71.2	652	12.59	22	1.88	28.24	783.71
Cc 21							720	2.45	13	0.28	1	0.05	73.32	
Cc 31							792	5.2	15	0.58	1	0.13	58.71	627.04
Cpx 21				147.6	1	152.3	91	1.86	7	0.86	1	0.41	8.14	17.61
Cpx 31				129.9	0.7	173.5	95	1.56	6	0.54	1	0.39	11.85	16.45
Mel 21	28.7	15.5	1.9	1 907.2	10.9	175.7	965	19.71	677	86.45	193	98.3	0.18	0.4
Mel 31	22.2	10.9	2	1 220.3	5.5	220.7	814	21.39	555	85.71	142	97.99	0.17	0.44
Nep 21	0.6	0.2	3				87	1.78	5	0.6	0	0.16	14.66	188.03
Nep 31	0.6	0.2	3				52	0.17	6	0.12	1	0.08		
WR 21	56.6	7.1	7.9	616.5	3.5	173.8	1 469		235		59		3.74	9.28
WR 31	62.6	7.2	8.7	520.6	2.4	218.1	1 523		259		58		3.27	8.97

Note: Concentrations are presented in ppm; the whole-rock data are calculated based on mineral mol% in Chen and Simonetti, 2013.

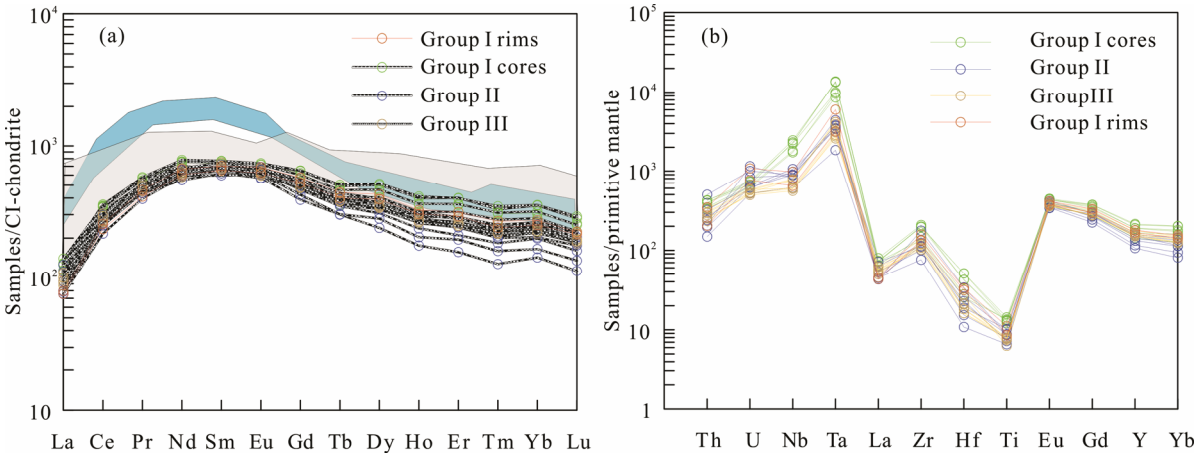

Figure 5. Chondrite normalized REE distribution patterns (a) and primitive mantle (PM) normalized trace elements distribution patterns (b) for garnets from groups I, II and III. Chondrite values are referred to McDonough and Sun, 1995, and primitive mantle values are referred to Sun and McDonough, 1989. In REE distribution plots, patterns for Ti-garnets from Sung Valley (grey; Melluso et al., 2010) and Alno Island (blue; Vuorinen et al., 2005) are presented as a comparison.

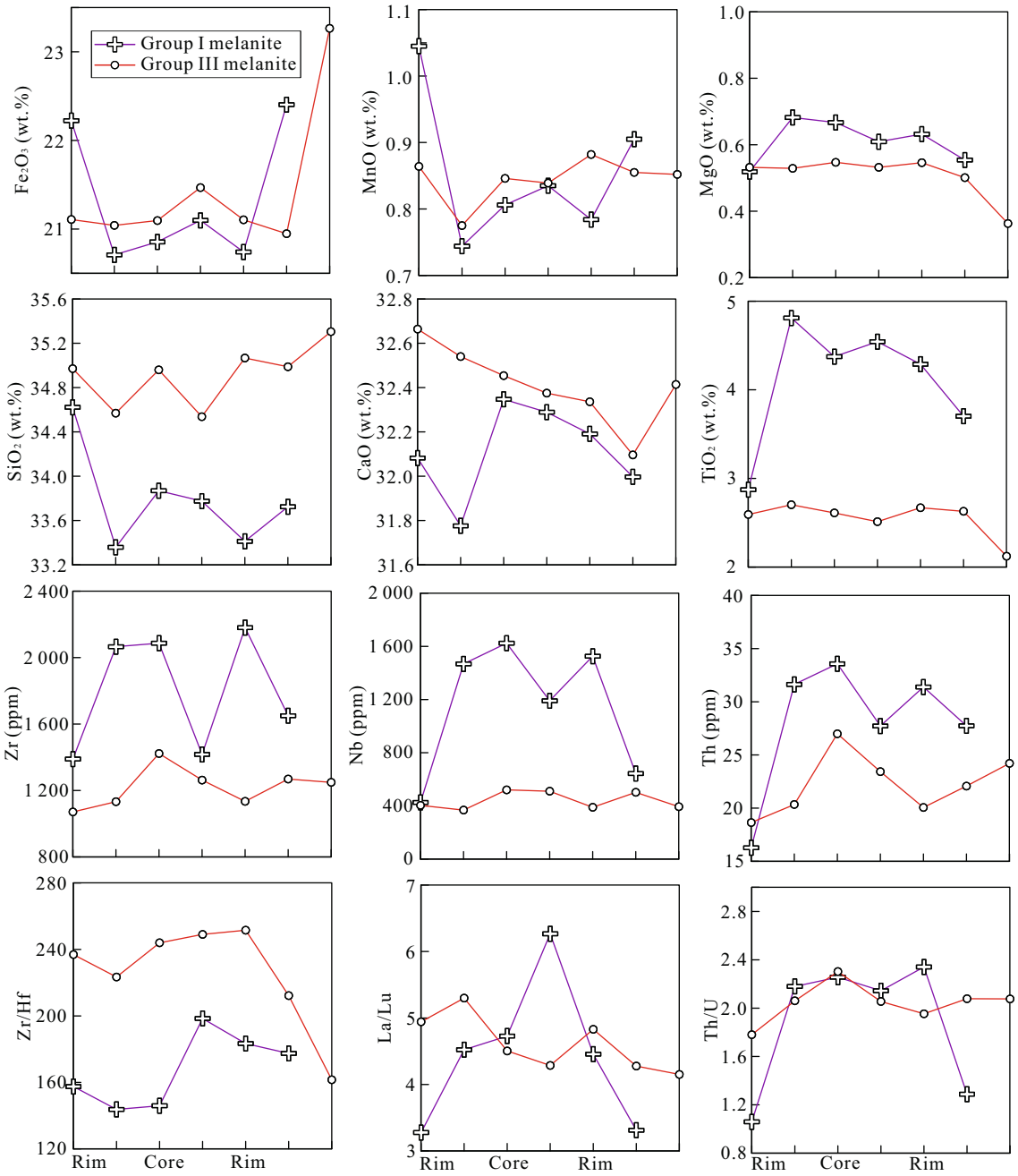

Figure 6. Compositional profiles for zoned garnets from Oka21 and Oka31.

calcite, apatite, nepheline and clinopyroxene; Chen and Simonetti, 2013; Table 3), garnet contains higher abundances of MREEs (middle REEs) and HREEs and is relatively depleted in LREEs (e.g., $(La/Gd)_N$=~0.17; $(La/Lu)_N$= ~0.40; Table 3). Of note, the HREEs are especially enriched with more than 100 times chondrite values (Fig. 5a). Based on the modal distribution and REE contents of the rock-forming minerals (e.g., garnet, clinopyroxene, calcite and apatite), REE distributions for these minerals from calcitic ijolite are presented in Table 3. The results suggest that melanite garnet accounts for 98% HREEs, 85% MREEs, and 20% LREEs of the calcitic ijolite whole rock (Table 3). Thus, melanite fractionation can significantly decrease the calcitic ijolite whole-rock HREE as well as MREE abundances, and affect the REE distributions in the co-crystallized or later-formed mineral phases (e.g., clinopyroxene, calcite, apatite, and nepheline). For instance, as shown in Chen and Simonetti (2013), apatite from calcitic ijolite is characterized by the highest $(La/Yb)_N$ ratio compared to other rock types (e.g., carbonatite, okaite) at Oka.

Moreover, melanite contains high abundances of HFSEs (e.g., Zr, Hf, Th, U), and it is one of the major minerals that dominate the HFSE budget of the whole rock. For example, melanite contains the highest amounts of Zr (1 071 ppm– 2 586 ppm) and Hf (4.5 ppm–14.4 ppm; Table 2); the latter are ~10 times higher compared to those in clinopyroxene, which is the other potential HFSE host within calcitic ijolite (Table 3). Thus, melanite is the predominant mineral controlling the Zr/Hf ratio (budget) for calcitic ijolite. Significantly higher Zr/Hf ratios are observed for groups II and III garnet relative to Group I garnet (Fig. 8a), which may imply crystallization from two different

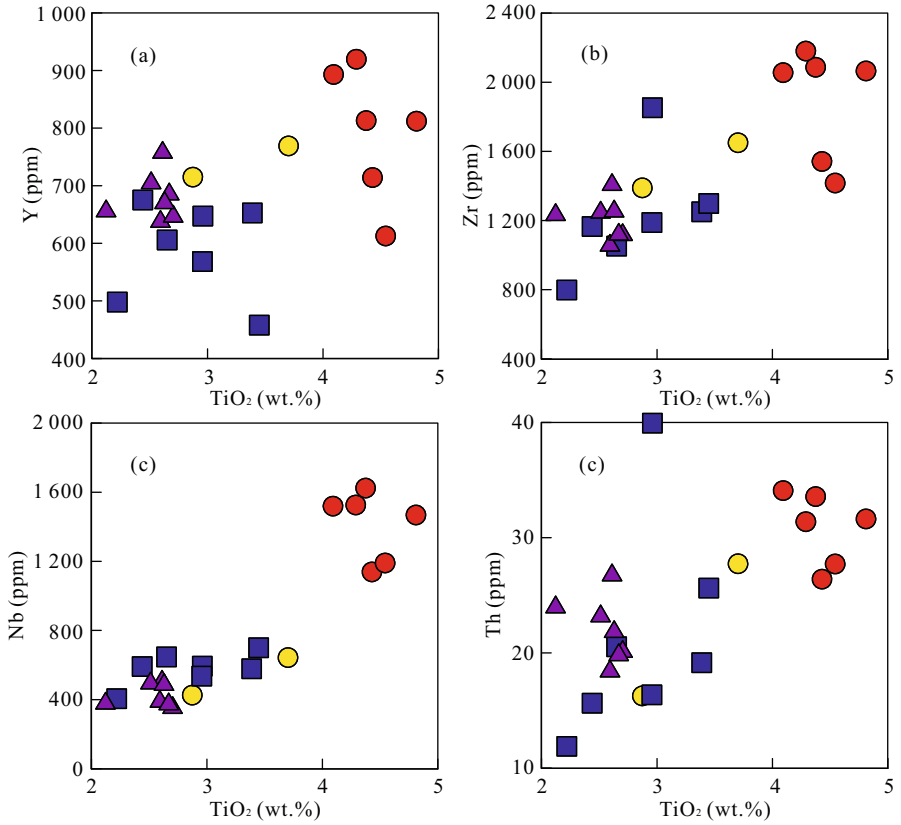

Figure 7. Plots exhibiting the correlation between Y (a), Zr (b), Nb (c), Th (d) and TiO_2. Legends are the same as those adopted in Fig. 4.

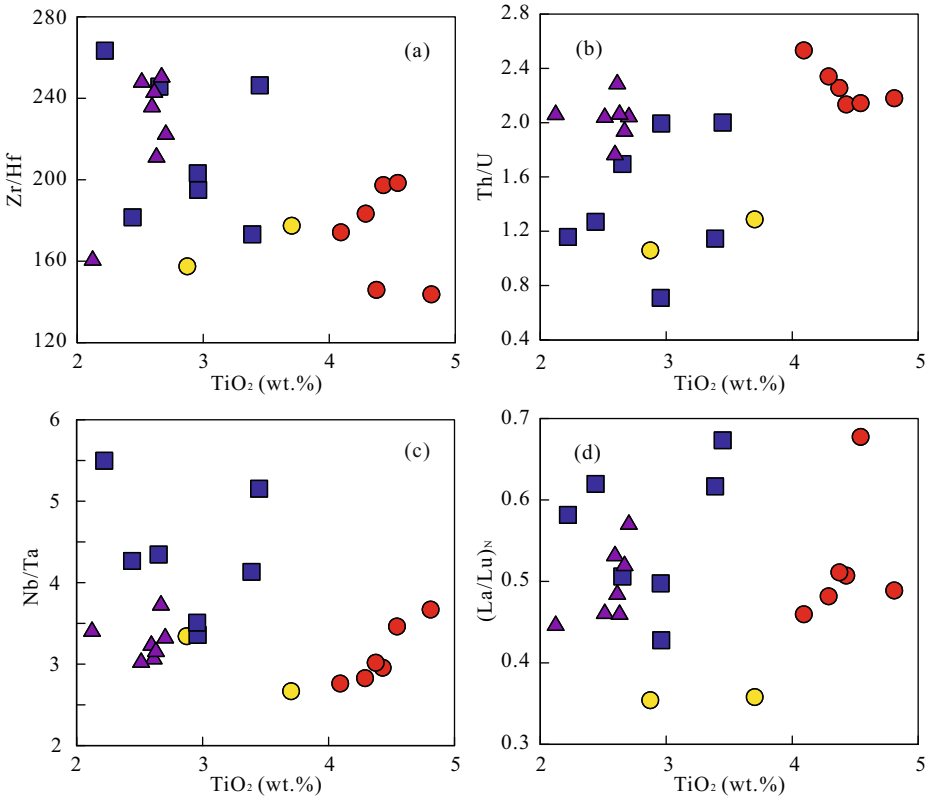

Figure 8. Composition variation diagrams for garnet from different groups. (a) Zr/Hf v.s. TiO_2; (b) Th/U v.s. TiO_2; (c) Nb/Ta v.s. TiO_2; (d) $(La/Yb)_N$ v.s. TiO_2. Legends are the same as those adopted in Fig. 4.

magmas with distinct Zr/Hf compositions. This is not consistent with a simple either slow fractional crystallization in a magma chamber under high pressure and temperature or fast fractional crystallization during eruption or at shallow depth. Similar variation trends could have been identified for Nb/Ta (Fig. 8c), whereas Group II garnet are characterized by higher Nb/Ta ratios compared to the remaining. The Th and U abundances for Oka melanite are between 15.6 ppm–40.5 ppm and 9.9 ppm–21.5 ppm, respectively, and the Th/U ratio ranges from 1.1 to 2.5 (Table 3). As shown in Fig. 8b, Group I garnet rim and Group II garnet show lower Th/U ratios compared to those for Group I garnet core and Group III. Of note, apatite is the mineral within calcitic ijolite that contains the highest Th (956 ppm–1 071 ppm) and U (48.6 ppm–55.5 ppm) contents (Table 3). It consists of much higher Th/U ratios (19.3–19.7; Table 3) compared to that for melanite. Thus, apatite is the dominant mineral that fractionates Th/U ratio in the calcitic ijolite magma, i.e., fractionation of apatite will significantly decrease the Th/U of the residual melt. Hence, the crystallization of apatite, as demonstrated by its presence as inclusions within the Group I garnet rims, may contribute to the lower Th/U ratios compared to Group I garnet cores. Alternatively, it is possible that these two distinct chemical garnet groups crystallized from two different magmas. In addition, higher Th/U ratios have been observed for Group III compared to Group II and Group I rim garnets, which suggests generation from distinct magmas with different Th/U ratios. Group I rim garnets contain lower $(La/Lu)_N$ ratios compared to those for the core (Fig. 8d), whereas the ratios should increase from core to rim in a simple fractional crystallizaiton process as garnet serves as the dominant mineral that fractionates the HREEs (Table 3; Marks et al., 2008). Hence, it is consistent with open system behavior involving more than one parental magma sources.

4.2 Petrogenetic History for Calcitic Ijolite

Group I garnet shows the most distinct chemical zonation, which reflects a chemical transition between core and rim. The decrease of TiO_2 contents from core-to-rim is similar to those observed in alkaline complexes elsewhere (e.g., Melluso et al., 1996; Barbiebi et al., 1987). The distinct compositions between rim and core are reflected in both major (e.g., Ti, Si, Fe, Mg), trace element (e.g., REEs, Zr, Hf, U) abundances and elemental ratios (e.g., Th/U, La/Lu). This distinct chemical and petrographic zoning cannot be simply interpreted as the result of a closed system crystallization, but most likely involves multi-pulse magma mixing. Melt differentiation involving continuous fractional crystallization cannot produce the abrupt changes in major and trace element abundances as shown by the core-to-rim grain traverses (Fig. 6). The dark colored inner Group I garnet cores show distinct petrographic and mineralogical features compared to Group I rim and groups II and III garnets (Fig. 2), which further supports mixing with a new batch of magma. In addition, complicated trace element variation trend have been observed for these garnets (Fig. 8), e.g., groups II and III garnets are characterized by distinct Zr/Hf and Nb/Ta ratios that indicates crystallization from a different magma source. Group III garnet with fine oscillatory zonation shows limited chemical variations compared to that of Group I, and no trends are recorded for the zoned garnet, which might have resulted from a period of fluctuating P-T-f_{O2} similar to the oscillatory zonation observed within crystal I garnet from Amba Dongar (Gwalani et al., 2000; Ivanova et al., 1998), or possibly have been formed by continuous fractional crystallization (Antao et al., 2015).

The absence of mineral inclusions in the Group I core suggests an earlier crystallization event prior to that for the other rock-forming minerals (e.g., clinopyroxene, calcite, nepheline, and apatite). The remaining minerals are commonly included within Group I melanite rim, whereas melanite has been identified as inclusions within clinopyroxene. This indicates the co-crystallization of melanite rim and clinopyroxene and possibly nepheline, calcite, and apatite as well. Melanite can form over a wide range of temperature and pressure in alkaline rocks, and possibly reflects late-stage metasomatic reactions of earlier formed mafic minerals with fluids (e.g., Saha et al., 2011; Flohr and Ross, 1989). The late-stage metasomatic phases commonly observed in ijolite and associated alkaline rocks include cancrinite, natrolite, calcite, biotite, sodicpyroxnenes, K-feldspar and fluoro-hydrogradite (Flohr and Ross, 1989; Le Bas, 1977), which are rarely observed in the Oka calcitic ijolite. Nepheline in the matrix of calcitic ijolite is altered into cancrinite. However, other secondery minerals formed as the result of reaction between magmatic phases and metasomatic fluids such as natrolite, biotite, sodic pyroxenes. K-feldspar have not been observed in the ijolites. These melanites investigated for Oka are associated with mostly rock-forming magmatic minerals (i.e., apatite, magnetite, nepheline, diopside and calcite). Hence, late-stage metasomatism does not play a key role in the formation of the melanite.

Apatite included within Group III garnet yielded a distinct older U-Pb age (127±3.6 Ma) compared to apatite within the matrix (115±5.1 Ma; Chen and Simonetti, 2013); this implies that apatite, calcite, clinopyroxene, and nepheline continued crystallizing during the later stages of the complex's formational history. Overall, the crystallization sequence of the mineral phases within calcitic ijolite can be summarized as follows: (1) the first generation of Group I garnet core, either crystallization from the parental magma or cumulates from a different magma; (2) garnet within Group I rim and groups II & III crystallized from the more evolved magma together with the crystallization of some clinopyroxene, apatite, calcite, and nepheline; (3) calcite, nepheline, pyroxene, and apatite continue crystallizing to the late stage, which is coincident with the major pulse of the carbonatite formation at Oka (~114 Ma; Chen and Simonetti, 2014, 2013).

Magma mixing is commonly proposed to explain the non-equilibrium textures in alkaline magmatic rocks (i.e., chemical zonation and non-equilibrium mineral assemblage; Vuorinen et al., 2005; Gwalani et al., 2000; Simonetti et al., 1996; Simonetti and Bell, 1995, 1993; Sparks et al., 1977). At Oka, the extreme chemical variations documented by calcite, apatite, perovskite and pyrochlore as well as the complex zonation recorded by these minerals suggest open-system behavior and can be best explained by periodic generation of small volume melts and subsequent magma mixing (Chen and Simonetti, 2014, 2013; Chen et al., 2013; Zurevinski and Mitchell, 2004). The two perovskite

groups with different Nb abundances document distinct chemical, geochronological and isotopic information, which indicates that the Nb-E perovskite formed from an enriched melt produced at ~135 Ma and the Nb-D perovskite generated later at ~114 Ma from a less-enriched magma (Chen and Simonetti, 2014). The zoned garnet as discussed above indicates that the Group I core formed early from a melt characterized by low Si and high Ti activities, which mixed with a more depleted melt that generated Group I rim and groups II and III garnets (e.g., depleted in Ti, REEs, HFSEs). Some early-occurred apatite, pyroxene, nepheline, and calcite crystallized with the second generation of these garnets as evidenced by the co-mingled inclusions within each other. The corresponding age of the more evolved melt is recorded by apatite included in Group III at 127±3.6 Ma (Chen and Simonetti, 2013). Of note, the rest apatite in the calcitic ijolite matrix surrounded by calcite, nepheline, and pyroxene recorded a younger age at 115±5.1 Ma (Chen and Simonetti, 2013). The latter is coincident with the late stage crystallization of calcite, apatite, pyroxene, and nepheline from an even more evolved melt with increasing enrichment in CO_2 (Chen and Simonetti, 2014).

5 CONCLUSION

Multi-stage crystallization has been recorded in melanite from calcitic ijolite based on their petrographic and chemical signatures. The melt that generated Group I garnet cores was later mixed with at least two small-volume, more evolved melts. One formed the remaining garnet with early-formed pyroxene, calcite, nepheline, and apatite at 127±3.6 Ma. The more evolved melt crystallized the majority of pyroxene, calcite, nepheline, and apatite at 115±3.1 Ma. Hence, generation of calcitic ijolite at Oka resulted from at least three distinct pluses of magma and subsequent mixing, as recorded by the chemical and petrographic evidences exhibited by melanite garnet.

ACKNOWLEDGMENTS

We thank Ian Steele, University of Chicago Electron Microprobe Laboratory, for his assistance with EMP data collection. This study was supported by the National Natural Science Foundation of China (No. 41402046), the Fundamental Research Funds for the Central Universities (No. 2015219102) and the special fund from the State Key Laboratory of Geological Processes and Mineral Resources. Haijin Xu and an anonymous reviewer are warmly thanked for their constructive and thoughtful comments. Wei Chen gratefully acknowledges receiving financial support during her doctoral dissertation from the University of Notre Dame. The final publication is available at Springer via http://dx.doi.org/10.1007/s12583-016-0715-3.

REFERENCES CITED

Antao, S. M., Mohib, S., Zaman, M., et al., 2015. Ti-Rich Andradites: Chemistry, Structure, Multi-Phases, Optical Anisotropy, and Oscillatory Zoning. *The Canadian Mineralogist*, 53(1): 133–158. doi:10.3749/canmin.1400042

Armbruster, T., Birrer, J., Libowitzky, E., et al., 1998. Crystal Chemistry of Ti-Bearing Andradites. *European Journal of Mineralogy*, 10(5): 907–922

Barbieri, M., Beccaluva, L., Brotzu, P., et al., 1987. Petrological and Geochemical Studies of Alkaline Rocks from Continental Brazil. 1. The Phonolite Suite from Piratini, RS. *Geochimica Brasiliensis*, 1: 109–138

Chakhmouradian, A. R., McCammon, C. A., 2005. Schorlomite: A Discussion of the Crystal Chemistry, Formula, and Inter-Species Boundaries. *Physics and Chemistry of Minerals*, 32(4): 277–289. doi:10.1007/s00269-005-0466-7

Chen, W., Simonetti, A., 2013. In-Situ Determination of Major and Trace Elements in Calcite and Apatite, and U-Pb Ages of Apatite from the Oka Carbonatite Complex: Insights into a Complex Crystallization History. *Chemical Geology*, 353: 151–172. doi:10.1016/j.chemgeo.2012.04.022

Chen, W., Simonetti, A., Burns, P. C., 2013. A Combined Geochemical and Geochronological Investigation of Niocalite from the Oka Carbonatite Complex, Canada. *The Canadian Mineralogist*, 51(5): 785–800. doi:10.3749/canmin.51.5.785

Chen, W., Simonetti, A., 2014. Evidence for the Multi-Stage Petrogenetic History of the Oka Carbonatite Complex (Québec, Canada) as Recorded by Perovskite and Apatite. *Minerals*, 4(2): 437–476. doi:10.3390/min4020437

Davidson, A., Gold, D. P., Union, C. G., 1986. Carbonatites, Diatremes and Ultra-Alkaline Rocks in the Oka Area, Quebec. Geological Association of Canada

Dawson, J. B., Smith, J. V., Steele, I. M., 1995. Petrology and Mineral Chemistry of Plutonic Igneous Xenoliths from the Carbonatite Volcano, Oldoinyo Lengai, Tanzania. *Journal of Petrology*, 36(3): 797–826. doi:10.1093/petrology/36.3.797

Dawson, J., 1998. Peralkaline Nephelinite-Natrocarbonatite Relationships at Oldoinyo Lengai, Tanzania. *Journal of Petrology*, 39(11): 2077–2094. doi:10.1093/petrology/39.11.2077

Deer, W. A., Howie, R. A., Zussman, J., 1982. Rock-Forming Minerals: Orthosilicates, Volume 1A. Geological Society of London, London

Dingwell, D. B., Brearley, M., 1985. Mineral Chemistry of Igneous Melanite Garnets from Analcite-Bearing Volcanic Rocks, Alberta, Canada. *Contributions to Mineralogy and Petrology*, 90(1): 29–35. doi:10.1007/bf00373038

Dunworth, E. A., Bell, K., 2003. The Turiy Massif, Kola Peninsula, Russia: Mineral Chemistry of an Ultramafic-Alkaline-Carbonatite Intrusion. *Mineralogical Magazine*, 67(3): 423–451. doi:10.1180/0026461036730109

Eby, G. N., 1975. Abundance and Distribution of the Rare-Earth Elements and Yttrium in the Rocks and Minerals of the Oka Carbonatite Complex, Quebec. *Geochimica et Cosmochimica Acta*, 39(5): 597–620. doi:10.1016/0016-7037(75)90005-8

Flohr, M. J., Ross, M., 1989. Alkaline Igneous Rocks of Magnet Cove, Arkansas: Metasomatized Ijolite Xenoliths from Diamond Jo Quarry. *American Mineralogist*, 74(1/2): 113–131

Gold, D. P., 1972. The Monteregian Hills: Ultra-Alkaline Rocks and the Oka Carbonatite Complex. 24th International Geological Congress Guidebook B-11, Montreal

Gold, D. P., Eby, G. N., Bell, K., et al., 1986. Carbonatites, Diatremes and Ultra-Alkaline Rocks in the Oka Area,

Quebec. Geological Association of Canada Guidebook, Ottawa

Gwalani, L. G., Rock, N. M. S., Ramasamy, R., et al., 2000. Complexly Zoned Ti-Rich Melanite-Schorlomite Garnets from Ambadungar Carbonatite-Alkalic Complex, Deccan Igneous Province, Gujarat State, Western India. *Journal of Asian Earth Sciences*, 18(2): 163–176. doi:10.1016/s1367-9120(99)00053-x

Holub, F. V., Rapprich, V., Erban, V., et al., 2010. Petrology and Geochemistry of the Tertiary Alkaline Intrusive Rocks at Doupov, Doupovské Hory Volcanic Complex (NW Bohemian Massif). *Journal of Geosciences*, 55: 251–278. doi:10.3190/jgeosci.074

Huggins, F., Virgo, D., Huckenholz, H., 1977a. Titanium-Containing Silicate Garnet: I, The Distribution of Al, Fe^{3+}, and Ti^{4+} between Octahedral and Tetrahedral Sites. *American Mineralogist*, 62(5/6): 475–490

Huggins, F., Virgo, D., Huckenholz, H., 1977b. Titanium-Containing Silicate Garnets: II, The Crystal Chemistry of Melanites and Schorlomites. *American Mineralogist*, 62(7/8): 646–665

Ivanova, T., Shtukenberg, A., Punin, Y. O., et al., 1998. On the Complex Zonality in Grandite Garnets and Implications. *Mineralogical Magazine*, 62(6): 857–868

Le Bas, M. J., 1977. Carbonatite-Nephelinite Volcanism: An African Case History. John Wiley & Sons

Locock, A. J., 2008. An Excel Spreadsheet to Recast Analyses of Garnet into End-Member Components, and a Synopsis of the Crystal Chemistry of Natural Silicate Garnets. *Computers & Geosciences*, 34(12): 1769–1780. doi:10.1016/j.cageo.2007.12.013

Locock, A., Luth, R. W., Cavell, R. G., et al., 1995. Spectroscopy of the Cation Distribution in the Schorlomite Species of Garnet. *American Mineralogist*, 80(1/2): 27–38. doi:10.2138/am-1995-1-204

Maitra, M., David, J. S., Bhaduri, S., 2011. Melanite Garnet-Bearing Nepheline Syenite Minor Intrusion in Mawpyut Ultramafic-Mafic Complex, Jaintia Hills, Meghalaya. *Journal of Earth System Science*, 120(6): 1033–1041. doi:10.1007/s12040-011-0129-7

Manning, P., Harris, D., 1970. Optical-Absorption and Electron-Microprobe Studies of Some High-Ti Andradites. *The Canadian Mineralogist*, 10(2): 260–271

Marks, M., Coulson, I., Schilling, J., et al., 2008. The Effect of Titanite and Other HFSE-Rich Mineral (Ti-Bearing Andradite, Zircon, Eudialyte) Fractionation on the Geochemical Evolution of Silicate Melts. *Chemical Geology*, 257(1/2): 153–172. doi:10.1016/j.chemgeo.2008.09.002

McDonough, W. F., Sun, S. S., 1995. The Composition of the Earth. *Chemical Geology*, 120(3/4): 223–253. doi:10.1016/0009-2541(94)00140-4

Melluso, L., Morra, V., Di Girolamo, P., 1996. The Mt. Vulture Volcanic Complex (Italy): Evidence for Distinct Parental Magmas and for Residual Melts with Melilite. *Mineralogy and Petrology*, 56(3/4): 225–250. doi:10.1007/bf01162605

Melluso, L., Srivastava, R. K., Guarino, V., et al., 2010. Mineral Compositions and Petrogenetic Evolution of the Ultramafic-Alkaline-Carbonatitic Complex of Sung Valley, Northeastern India. *The Canadian Mineralogist*, 48(1): 205–229. doi:10.3749/canmin.48.1.205

Niu, H. C., Zhang, H. X., Shan, Q., et al., 2008. Discovery of Super-Silicic and Super-Titanic Garnets in Garnet-Pyroxenite in Zhaheba and Its Geological Significance. *Science Bulletin*, 53(14): 2186–2191. doi:10.1007/s11434-008-0280-y

Russell, J. K., Dipple, G. M., Lang, J. R., et al., 1999. Major-Element Discrimination of Titanian Andradite from Magmatic and Hydrothermal Environments: An Example from the Canadian Cordillera. *European Journal of Mineralogy*, 11(6): 919–936. doi:10.1127/ejm/11/6/0919

Saha, A., Ray, J., Ganguly, S., et al., 2011. Occurrence of Melanite Garnet in Syenite and Ijolite-Melteigite Rocks of Samchampi-Samteran Alkaline Complex, Mikir Hills, Northeastern India. *Curr. Sci.*, 101: 95–100

Simonetti, A., Bell, K., 1993. Isotopic Disequilibrium in Clinopyroxenes from Nephelinitic Lavas, Napak Volcano, Eastern Uganda. *Geology*, 21(3): 243–246. doi:10.1130/0091-7613(1993)021<0243:idicfn>2.3.co;2

Simonetti, A., Bell, K., 1995. Nd, Pb and Sr Isotopic Data from the Mount Elgon Volcano, Eastern Uganda-Western Kenya: Implications for the Origin and Evolution of Nephelinite Lavas. *Lithos*, 36(2): 141–153. doi:10.1016/0024-4937(95)00011-4

Simonetti, A., Shore, M., Bell, K., 1996. Diopside Phenocrysts from Nephelinite Lavas, Napak Volcano, Eastern Uganda: Evidence for Magma Mixing. *The Canadian Mineralogist*, 34(2): 411–421

Sparks, S. R. J., Sigurdsson, H., Wilson, L., 1977. Magma Mixing: A Mechanism for Triggering Acid Explosive Eruptions. *Nature*, 267(5609): 315–318. doi:10.1038/267315a0

Sun, S. S., McDonough, W. F., 1989. Chemical and Isotopic Systematics of Oceanic Basalts: Implications for Mantle Composition and Processes. *Geological Society*, *London*, *Special Publications*, 42(1): 313–345. doi:10.1144/gsl.sp.1989.042.01.19

Treiman, A. H., Essene, E. J., 1985. The Oka Carbonatite Complex, Quebec: Geology and Evidence for Silicate-Carbonate Liquid Immiscibility. *American Mineralogist*, 70(11/12): 1101–1113

Van Achterbergh, E., Ryan, C., Jackson, S., et al., 2001. Data Reduction Software for LA-ICP-MS. *Laser-Ablation-ICPMS in the Earth Sciences—Principles and Applications. Miner Assoc Can* (*Short Course Series*), 29: 239–243

Vuorinen, J. H., Hålenius, U., Whitehouse, M. J., et al., 2005. Compositional Variations (Major and Trace Elements) of Clinopyroxene and Ti-Andradite from Pyroxenite, Ijolite and Nepheline Syenite, Alnö Island, Sweden. *Lithos*, 81(1–4): 55–77. doi:10.1016/j.lithos.2004.09.021

Zurevinski, S. E., Mitchell, R. H., 2004. Extreme Compositional Variation of Pyrochlore-Group Minerals at the Oka Carbonatite Complex, Quebec: Evidence of Magma Mixing? *The Canadian Mineralogist*, 42(4): 1159–1168. doi:10.2113/gscanmin.42.4.1159